Symmetrical and Unsymmetrical Quadruply Aza-Bridged Closely Interspaced Cofacial Bis(5,10,15,20-Tetraphenylporphyrins). 4. Structure and Conformational Effects on Electrochemistry and the Catalysis of Electrochemical Reduction of Dioxygen by Doubly, Triply, and Quadruply *N,N*-Dimethylene Sulfonamide Bridged Dimeric Bis(cobalt tetraphenylporphyrins)

Seungwon Jeon, Örn Almarsson, Rafik Karaman, Andrei Blaskó, and Thomas C. Bruice*

Department of Chemistry, University of California at Santa Barbara, Santa Barbara, California 93106

Received November 25, 1992

Investigations of the structural and electrochemical properties of free base, bis(zinc), and bis(cobalt) derivatives of a number of quadruply, as well as doubly and triply, *N,N*-dimethylene sulfonamide bridged cofacial bis(5,10,15,20-tetraphenylporphyrins) (Chart II) were conducted. The solution structure of [3-pyridyl]$_4$, determined by 2D NMR spectroscopy and distance geometry refinement, differs little from the gas-phase structure calculated by molecular mechanics. The ^{1}H NMR chemical shifts of the N–H pyrrolic protons (in $CDCl_3$ at 25 °C) of the quadruply bridged dimers [1-naphthyl]$_4$, [3-pyridyl]$_4$, [isopropyl]$_4$, and [methyl]$_4$ are linearly related to Taft's E_S steric parameters for the R substituent (=naphthyl, phenyl, isopropyl, and methyl) of the *N,N*-dimethylene sulfonamide bridges [$(-CH_2)_2NSO_2R$]. The results show that the center to center distances of the bis(porphyrins) decrease with increasing steric demands of R. For the bis(porphyrin) with the largest R substituent ([1-napthyl]$_4$), potentials for electrochemical oxidations of both the free base and bis(zinc) derivative establish a strong π–π interaction between the cofacial porphyrin rings. In the catalysis of the electrochemical reduction of O_2 the cobalt(II)-ligated bis(porphyrins) may be divided into two groups, with the neutral dimers Co_2–[methyl]$_4$, Co_2–[isopropyl]$_4$, and Co_2–[1-naphthyl]$_4$ exhibiting modest catalytic efficiencies in the 4e$^-$ reduction of dioxygen to water (between 44 and 51% H_2O), while the tetracationic porphyrin dimers {Co_2–[*N*-methyl-3-pyridyl$^+$]$_4$, Co_2–[*N*-isopropyl-3-pyridyl$^+$]$_4$, Co_2–[*N*-benzhydryl-3-pyridyl$^+$]$_4$, and tetraprotonated Co_2–[3-pyridyl·H$^+$]$_4$} are more effective (between 66 and 71% 4e$^-$ reduction). For the positively charged N-substituted pyridine dimers, the bulk of the N-substituents [$-CH_3$, $-CH(CH_3)_2$, $-CH(C_6H_5)_2$, –H] does not affect the catalytic properties nor Ct–Ct distances. With employment of the *N,N*-dimethylene sulfonamide bridging structures [$(-CH_2)_2NSO_2R$], the quadruply bridged tetracationic bis(cobalt) porphyrin dimer Co_2–[3-pyridyl·H$^+$]$_4$ is more effective in catalyzing the 4e$^-$ reduction of O_2 than are the two isomeric triply bridged and tricationic dimers Co_2–[3-pyridyl·H$^+$]$_3$(A) and Co_2–[3-pyridyl·H$^+$]$_3$(B) while the doubly bridged, dicationic Co_2–[3-pyridyl·H$^+$]$_2$ is the least active. Structural flexibility {[3-pyridyl]$_2$ > [3-pyridyl]$_3$(B) > [3-pyridyl]$_3$(A) > [3-pyridyl]$_4$} and the number of positive charges on the dimers account for the order of catalytic efficiency.

Introduction

A number of symmetrical and unsymmetrical quadruply bridged closely interspaced cofacial bis(5,10,15,20-tetraphenylporphyrins) have been synthesized in our laboratory and examined as catalysts for the 4e$^-$ reduction of dioxygen to water.[1] Geometrical parameters for the dimeric porphyrins (Chart I), such as the interplanar distance (P–P), the center to center distance (Ct–Ct), and the lateral shift (LS), as well as the shape of the cavity, appear to be determined by the conformation of the three atom *N,N*-dimethylene amine bridges.[1f,2]

In the present study, the Ct–Ct distance in the representative [3-pyridyl]$_4$ (see Chart II) has been made available by determination of its solution structure from two-dimensional ^{1}H NMR (ROESY) and subsequent distance geometry refinement. The solution structure is compared with the CHARM$_m$ calculated structure. Also described are the effect of the number of the bridges and the size and charge of their substituents on the electrochemical properties of both free base, bis(zinc), and bis(cobalt) derivatives as well as the catalysis of electrochemical reduction of oxygen by the latter.

Chart I

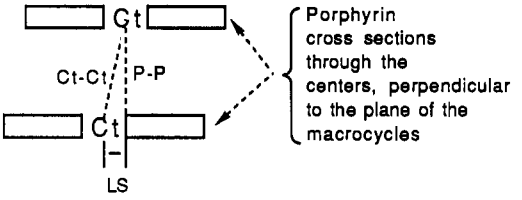

Results and Discussion

The structures of the quadruply bridged cofacial bis(5,10,15,20-tetraphenylporphyrins) of this study are shown in Chart II. For the *N,N*-dimethylene sulfonamide linker unit employed [$(-CH_2)_2NSO_2R$], the variation of Ct–Ct distance is dependent upon the identity of the R-group. The means by which substituent size determines interplanar distances[1f] is shown on inspection of the two structures of Chart III. The four legs which secure the two porphyrin rings can be considered to have a secondary nitrogen as a "knee". The knee is maximally extended (maximal Ct–Ct distance; a in Chart III) when the sulfonamide substituent is small, but as the bulk of the substituent becomes greater, van der

(1) (a) Abbreviations used: For a given bis(5,10,15,20-tetraphenylporphyrin) linked by *x N,N*-dimethylenesulfonamide linkages through the *m*-position of each *meso*-phenyl ring and carrying a group R on the sulfur atom, the suggested shorthand is [R]$_x$. Thus, the quadruply methanesulfonamide-linked dimer is referred to as [methyl]$_4$. Where more than one isomer exists, suffixes in parentheses, i.e. (A) and (B), are used for differentiation. (b) Bookser, B. C.; Bruice, T. C. *J. Am. Chem. Soc.* **1991**, *113*, 4208. (c) Karaman, R.; Bruice, T. C. *J. Org. Chem.* **1991**, *56*, 3470. (d) Karaman, R.; Blaskó, A.; Almarsson, Ö.; Arasasingham, R. D.; Bruice, T. C. *J. Am. Chem. Soc.* **1992**, *114*, 4889. (e) Karaman, R.; Jeon, S.; Almarsson, Ö.; Bruice, T. C. *J. Am. Chem. Soc.* **1992**, *114*, 4899. (f) Karaman, R.; Almarsson, Ö.; Bruice, T. C. *J. Org. Chem.* **1992**, *57*, 1555.

(2) (a) Chang, C. K.; Liu, H. Y.; Abdalmuhdi, I. *J. Am. Chem. Soc.* **1984**, *106*, 2725. (b) Collman, J. P.; Hendricks, N. H.; Leider, C. R.; Ngameni, E.; L'Her, M. *Inorg. Chem.* **1988**, *27*, 387. (c) Sawaguchi, T.; Matsue, T.; Itaya, K.; Uchida, I. *Electrochim. Acta* **1991**, *36*, 703. (d) Chang, C. K. *J. Heterocycl. Chem.* **1988**, *12*, 1287.

0020-1669/93/1332-2562$04.00/0

Chart II

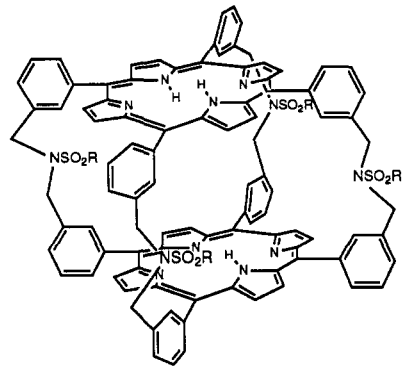

[N-methyl 3-pyridyl]$_4$ R = 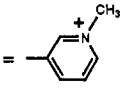

[3-pyridyl]$_4$ R = 

[methyl]$_4$ R = -CH$_3$

[N-isopropyl 3-pyridyl]$_4$ R = 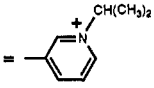

[isopropyl]$_4$ R = -CH(CH$_3$)$_2$

[N-benzhydryl 3-pyridyl]$_4$ R = 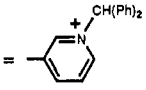

[1-naphthyl]$_4$ R = 

Chart III

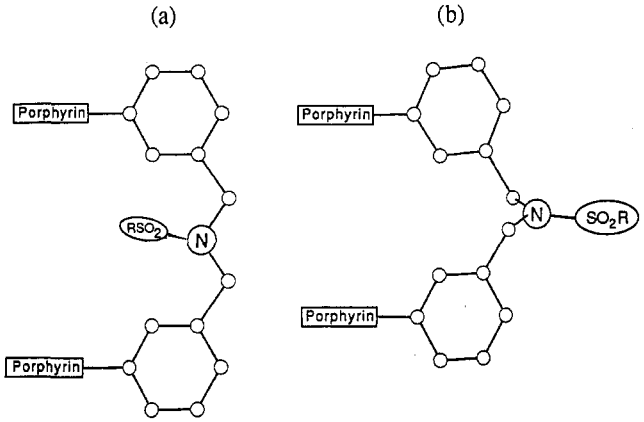

Waals repulsions exclude the substituent from the interplanar space and the knee begins to bend (providing decrease in Ct–Ct distance by a screwing down motion; b in Chart III). This conformational change becomes quite clear when viewed via computer graphics.[1f]

Effect of the Steric Bulk of the Sulfonamide R Substituent of the Quadruply Bridged Cofacial Bis(5,10,15,20-tetraphenylporphyrins) on the ^{1}H NMR Chemical Shifts of the Pyrrolic N–H Protons. In a previous investigation, using quadruply bridged cofacial porphyrins with varying "leg structures", we found[1f] that there exists a positive relationship between the size of the substituent on the secondary nitrogen "knee" (–CN, –CONH$_2$, –SO$_2$R) and the ^{1}H NMR chemical shift of the pyrrolic N–H protons. The upfield chemical shift of the pyrrolic N–H resonances for the dimers of this study (Chart II) are provided in Table I. With increased steric demands by substituent R the aforementioned ^{1}H NMR resonances shift upfield from corresponding signals for monomeric porphyrins due to the increased proximity of one porphyrin ring to the anisotropic ring current of the other porphyrin. This, again, speaks for decreased Ct–Ct distances in the free-base dimers with increased substituent size. Indeed, there is a good linear relationship between Taft's steric constants[3] (E_S) for the substituents R and the pyrrole proton NMR shifts (Figure 1).[4] Calculated CHARM$_m$ interplanar

Table I. Pyrrolic N–^{1}H Chemical Shifts (ppm vs TMS, at 500 MHz in $CDCl_3$ at 25 °C) and CHARM$_m$ calculated Ct–Ct[a] Distances (Å) for Quadruply *N,N*-Dimethylene Sulfonamide Bridged Free-Base Bis(5,10,15,20-tetraphenylporphyrins)

compd	δ(N–H)[a]	Ct–Ct[a]	E_S[b]
[1-naphthyl]$_4$	–4.68	4.88	–1.64
[3-pyridyl]$_4$	–4.34	5.03	–0.90[c]
[isopropyl]$_4$	–4.28	5.75	–0.47
[methyl]$_4$	–4.03	5.80	0.00

[a] See Chart I for definition of Ct–Ct and ref 1f for molecular dynamics protocol. [b] See footnote 3. [c] Parameter for phenyl rings.

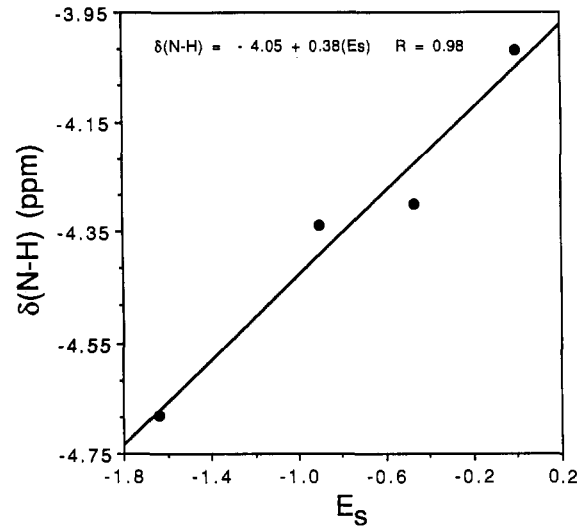

Figure 1. ^{1}H NMR pyrrolic N–H chemical shifts (at 500 MHz in $CDCl_3$ at 25 °C) vs E_S[3,4] for symmetrical quadruply *N,N*-dimethylene sulfonamide bridged free-base 5,10,15,20-tetraphenylporphyrin dimers [1-naphthyl]$_4$, [3-pyridyl]$_4$, [isopropyl]$_4$, and [methyl]$_4$. The E_S parameter for phenyl was used for the pyridine ring.

distances have been shown to have a reasonable linear correlation with ^{1}H NMR shifts[1e,1f] such that the E_S values of R-substituents on (–CH$_2$)$_2$NSO$_2$R should, therefore, be linearly related to Ct–Ct. The use of CHARM$_m$ to calculate Ct–Ct distances appears justified by the observation that CHARM$_m$ calculated distances agree closely with those determined by 2D ^{1}H NMR ROESY measurements, as shown in what follows.

Determination of a Solution Structure for [3-pyridyl]$_4$ by 2D NMR Spectroscopy and Distance Geometry Refinement. An expanded contour plot of the ROESY spectrum of [3-pyridyl]$_4$ in $CDCl_3$ solution is shown in Figure 2. With the usual assumption[5] that all proton–proton interactions can be described by the same correlation time, the ROESY peaks can be related to the sixth power of the distance between the protons involved in the interactions (see eq 4 in the Experimental Section). Using the fixed H5′-H6′ interatomic distance (2.46 Å) in [3-pyridyl]$_4$ as standard, the average distances for six types of interactions were calculated (Chart IV). A dihedral angle of approximately 20° between the phenyl rings and the porphyrin plane is required

(3) Taft, R. W. In *Steric Effects in Organic Chemistry*; Newman, M. S., Ed.; John Wiley: New York, 1976; p 598. E_S for 1-naphthyl was obtained from: Packer, J.; Vaughan, J.; Wong, E. *J. Org. Chem.* **1958**, *23*, 1373. The –0.40 value for acid-catalyzed ester hydrolysis was made relative to methyl by subtracting 1.24 to give –1.64.

(4) A similar relationship was observed between the pyrrolic N–H resonances and E_S of four unsymmetrical quadruply bridged dimers, where one of the sulfonamide linkers is replaced by a carbonate linkage.[1d,f] This unsymmetrical dimer series, isolated as byproducts in the synthesis of the symmetrical dimers, displays N–H resonances slightly downfield shifted compared with the symmetrical counterparts. The plot of N–H resonances vs E_S gives a modest linear correlation with a slope slightly smaller than that for the symmetrical series.

(5) (a) Kessler, H.; Bats, J. W.; Griesinger, C.; Koll, S.; Will, M.; Wagner, K. *J. Am. Chem. Soc.* **1988**, *110*, 1033. (b) Kessler, H.; Griesinger, C.; Kersebaum, R.; Wagner, E.: Ernst, R. *J. Am. Chem. Soc.* **1987**, *109*, 607.

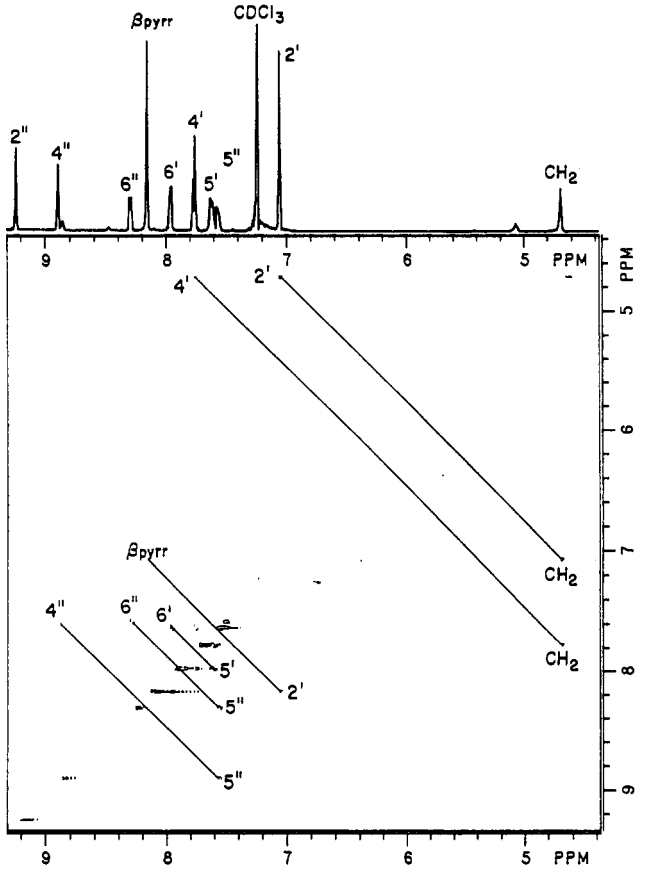

Figure 2. Expanded ROESY spectrum of porphyrin dimer [3-pyridyl]$_4$ on 500 MHz at 25 °C, in $CDCl_3$, with a mixing time of 200 ms and a spin locking field strength of 2.5 kHz.

Chart IV

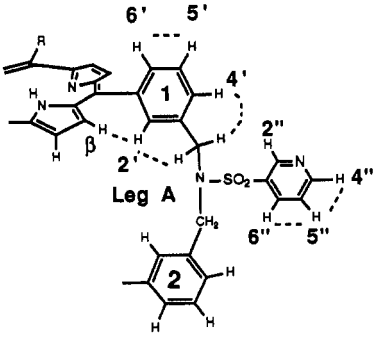

by the 2.40-Å distance between the H2′ of the phenyl rings and β-pyrrolic hydrogens. The orientation of the CH_2's and the phenyl rings is defined by the distance of 2.32 Å between CH_2 and H2′ and by the distance of 2.54 Å between CH_2 and H4′ (Chart IV). The relay constraints between the β-pyrrolic hydrogens, phenyl H2′, and CH_2's define the conformation of the legs and consequently the distance between the porphyrin planes.

For distance geometry (DGEOM)[7,15] calculations, an initial structure of [3-pyridyl]$_4$ was constructed using the program Quanta (MSI) and energy minimized in $CHARM_m$.[6] To this structure were added 24 distance constraints (8 times CH_2–H2′, CH_2–H4′, and β-pyrrolic–H2′) derived from the ROESY data (Table II). The upper limits for contact distances were set to be 10–15% higher than the NMR distances allowing the lower limit to be the van der Waals contact distances. The H6″–H5″ and H4″–H5″ distance constraints were not included because they

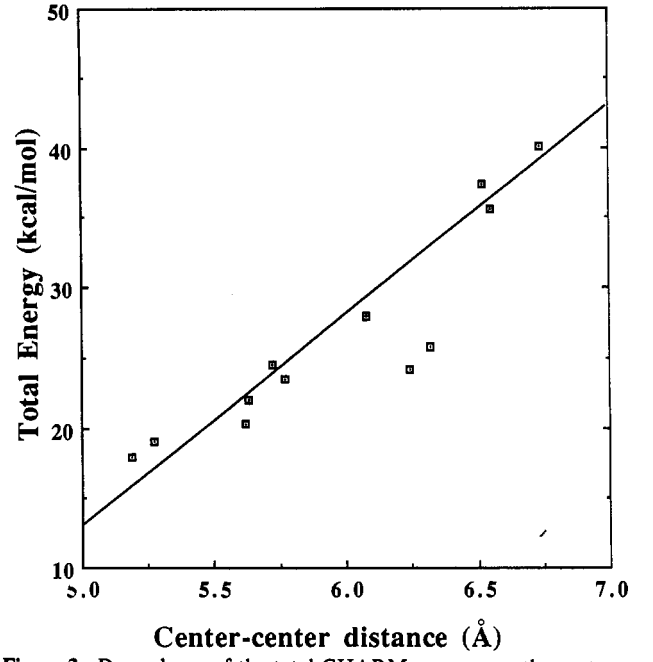

Figure 3. Dependence of the total $CHARM_m$ energy on the center to center (Ct–Ct) distances between the porphyrin rings in distance geometry refined ROESY structures for [3-pyridyl]$_4$.

Table II. ROESY (Exptl) and Most Stable Structure (Calcd) Interproton Distances (in Å) for [3-pyridyl]$_4$

			calcd			
H··H	exptl	ring	leg A	leg B	leg C	leg D
CH_2–H2′	2.32	1	2.51	2.45	2.55	2.43
		2	2.44	2.50	2.44	2.44
CH_2–H4′	2.54	1	2.49	2.86	2.47	2.61
		2	2.86	2.50	2.89	2.65
H2′–β (or β′)	2.40	1	3.32	3.18	3.13	3.46
		2	3.03	3.47	3.17	3.47
H5′–H6′	2.46	1	2.49	2.49	2.49	2.49
		2	2.49	2.49	2.49	2.49
H5″–H6″	2.52		2.50	2.50	2.50	2.50
H5″–H4″	3.17		2.50	2.50	2.50	2.50

belong to the pyridine ring and they have no significance in the calculations, although they are a measure of the accuracy of the ROESY–DGEOM method (Table II). One hundred conformers of [3-pyridyl]$_4$, which fit the ROESY constraints, were generated by use of the DGEOM program. The RMS matrix created by the DGEOM subprogram COMPARE was subjected to cluster analysis,[7] which grouped 100 conformers into 12 "families". A representative conformer was chosen from each "family" (by use of the statistical program Data Desk[8]) and energy minimized by $CHARM_m$. The spread in $CHARM_m$ energy content for the 12 minimized conformers was about 22 kcal/mol. Figure 3 shows a plot of the total $CHARM_m$ energy vs Ct–Ct distance for the 12 conformations which yields a modest linear correlation. The electrostatic and van der Waals terms from the force field[6] make the largest contributions to the total energy of the minimized conformers; the variation between structures lies mainly in the van der Waals term.

The ROESY distances and their refined values for the most stable conformer ($CHARM_m$ E_{total} = 17.9 kcal/mol) are shown in Table II, and the structure is shown in two stereoviews in Figure 4. The structure displays the shortest center to center distance, 5.19 Å, an interplanar distance of 5.17 Å, and lateral shift of 0.40 Å (see Chart I). The differences between the four sets of calculated H–H distances H2′–β and CH_2–H4′ are due

(6) Quanta, version 3.2; $CHARM_m$, version 21.3, from MSI, 1991. For a full description of the $CHARM_m$ force field, see: Brooks, B. R.; Bruccoleri, R. E.; Olafson, B. D.; States, D. J.; Swaminathan, S.; Karplus, M. *J. Comput. Chem.* **1983**, *4*, 187.

(7) Blaney, J. M.; Crippen, G. M.; Dearing, A.; Dixon, J. S. Du Pont de Nemours & Co., 1990.

(8) Data Desk, version 3.0, Odesta Corp., Northbrook, IL, 1989.

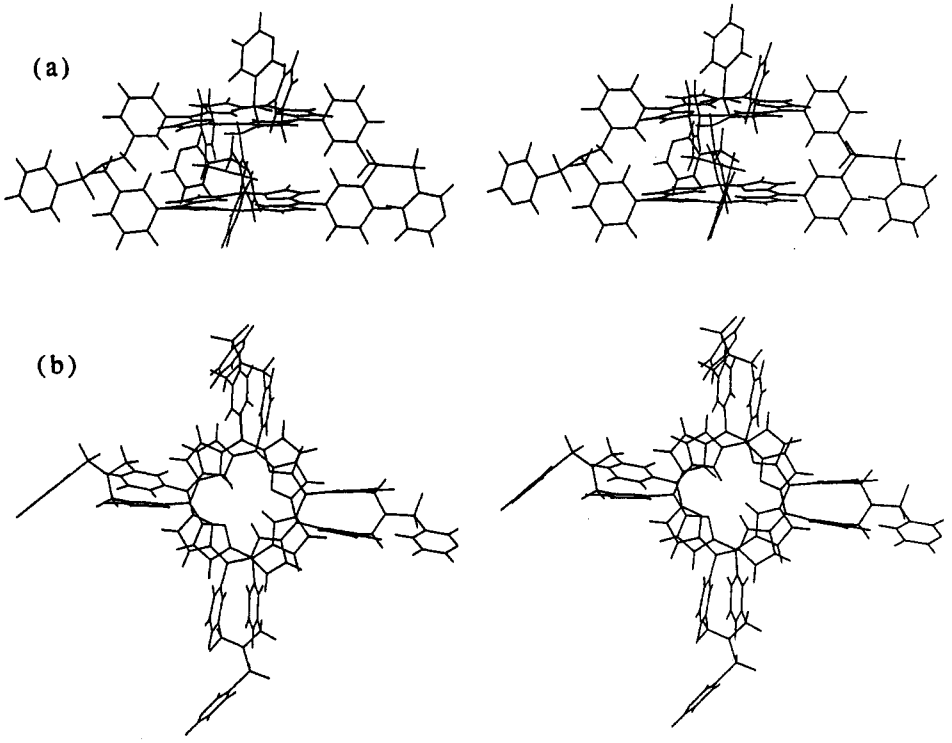

Figure 4. (a) Side view and (b) top view of stereo model for the most stable ($CHARM_m$) conformer of porphyrin dimer [3-pyridyl]$_4$ in $CDCl_3$ solution, determined by ROESY calculation and distance geometry refinement.

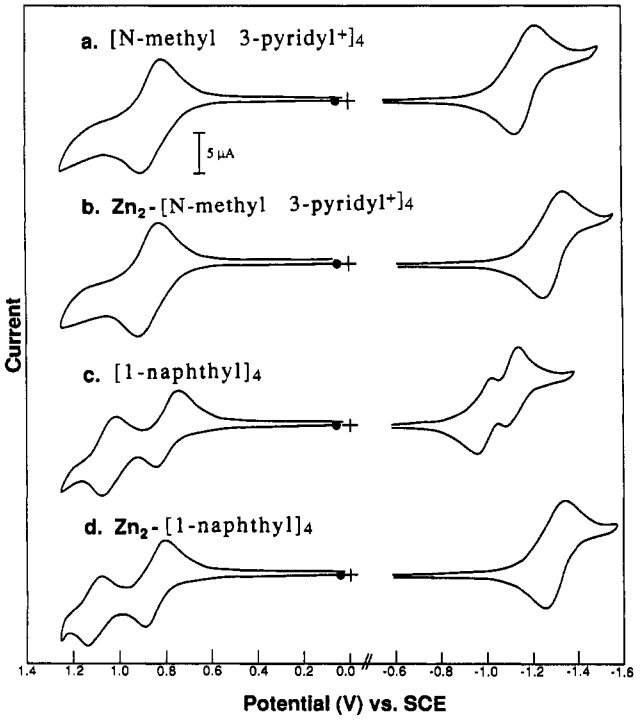

Figure 5. Cyclic voltammograms of the quadruply sulfonamide bridged cofacial tetraphenylporphyrins (a) [*N*-methyl-3-pyridyl$^+$]$_4$, (b) Zn_2–[*N*-methyl-3-pyridyl$^+$]$_4$, (c) [1-naphthyl]$_4$, and (d) Zn_2–[1-naphthyl]$_4$ in DMF, with supporting electrolyte 0.2 M Bu_4NBF_4, platinum electrode, and scan rate 0.1 V/s.

to the dissymmetry of the four pyridine moieties, which affects the folding of the legs, as well as the rotations of the *meso*-phenyl rings. The pyridine sulfonamides appear to posess considerable flexibility, according to molecular mechanics. Although the calculated solution structure for [3-pyridyl]$_4$ is not totally symmetric, an approximate D_4 symmetry is noted. As seen in Figure 4b, the structure displays a rotation of the porphyrin rings against each other by 20°. This staggering of the two rings is brought about by folding of the linkers between them (bending the "knees") and allows the porphyrin dimer to be quite compact in the $CDCl_3$ solution. The solution structure obtained by 2D NMR is in good agreement with the structure obtained[1f] by $CHARM_m$ energy minimization in the gas phase. Ct–Ct is less than 0.2 Å larger in the representative solution structure for [3-pyridyl]$_4$ than in its gas-phase structure,[1f] and a root mean square deviation of 0.8 Å is calculated for the difference between the porphyrin rings and bridges (excluding the 3-pyridylsulfonyl moieties). The difference in $CHARM_m$ total energies for the two structures is less than 2 kcal/mol.

Table III. Oxidation and Reduction Potentials for the Quadruply Sulfonamide Bridged Cofacial Tetraphenylporphyrins in DMF[a]

compd	E_{ox}^1 (V)[b]		E_{red}^1 (V)[c]	
1	+0.94		−1.20[d]	
[*N*-methyl-3-pyridyl$^+$]$_4$	+0.91		−1.18	
Zn_2–[*N*-methyl-3-pyridyl$^+$]$_4$	+0.94		−1.30	
[1-naphthyl]$_4$	+0.82	+1.07	−1.00	−1.09
Zn_2–[1-naphthyl]$_4$	+0.87	+1.15	−1.31	

[a] 0.1 M Bu_4NBF_4 was used as electrolyte, E (V) vs SCE. [b] First ring oxidation. [c] First ring reduction. [d] This peak indicates the irreversible reduction of the benzyl bromide attached to the meso positions of the porphyrin ring.

Electrochemistry of [*N*-methyl 3-pyridyl$^+$]$_4$ and [1-naphthyl]$_4$ and Their Bis(zinc) and Bis(cobalt) Derivatives in DMF. The electrochemistry of porphyrin complexes of nonelectroactive and electroactive metals has been studied extensively,[9] but relatively little is known about the electrochemical redox properties of free-base porphyrin dimers and metal porphyrin dimers containing redox-inactive metals.[10] Such information is required in order to seek a rational for metal porphyrin dimer structure vs electrochemical catalysis of $^3O_2$ reduction. Figure 5 shows typical

(9) Kadish, K. M. In *Progress in Inorganic Chemistry*; Lippard, S. J., Ed.; Wiley: New York, 1986; Vol. 34, p 435.
(10) (a) Becker, J. Y.; Dolphin, D.; Paine, J. B.; Wijesekera, T. *J. Electroanal. Chem. Interfacial Electrochem.* **1984**, *164*, 335. (b) Lexa, D.; Maillard, P.; Momenteau, M.; Saveant, J. M. *J. Am. Chem. Soc.* **1984**, *106*, 6321. (c) Osuka, A.; Maruyama, K. M. *Chem. Lett.* **1987**, 825. (d) Sessler, J. L.; Johnson, M. R.; Lin, T. Y.; Creager, *S. E. J. Am. Chem. Soc.* **1988**, *110*, 3659. (e) Mest, Y. L.; L'Her, M.; Hendricks, N. H.; Kim, K.; Collman, J. P. *Inorg. Chem.* **1992**, *31*, 835.

CV traces obtained in DMF for the free-base tetraphenylporphyrin dimers [*N*-methyl-3-pyridyl$^+$]$_4$ and [1-naphthyl]$_4$ and the corresponding bis(zinc) derivatives, Zn_2–[*N*-methyl-3-pyridyl$^+$]$_4$ and Zn_2–[1-naphthyl]$_4$, respectively. The well-defined waves represent quasi-reversible redox couples, as seen from the peak separation (ΔE_p) between the anodic and cathodic potentials. The peak current (i_p) is linearly dependent on the square root of the scan rate (v), as is expected for a diffusion-controlled process. The determined electrochemical potentials are shown in Table III. For comparison, the electrochemical potential of a monomeric porphyrin 5,10,15,20-tetrakis(α-bromo-*m*-tolyl)porphyrin (**1**) is

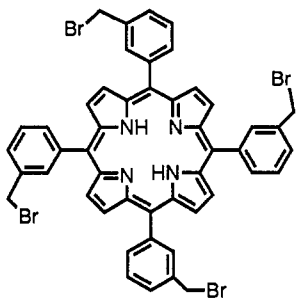

1

included in Table III. In CH_2Cl_2 solution **1** exhibits two oxidation waves at E_{ox}^1 = +1.14 V and at E_{ox}^2 = +1.37 V. In this solvent, **1** undergoes oxidation by two sequential 1e$^-$ transfers as depicted in eq 1. In contrast, a DMF solution of **1** shows one oxidation

$$MP \xrightarrow{-e^-} MP^{\bullet+} \xrightarrow{-e^-} MP^{2+} \qquad (1)$$

MP = monomeric tetraphenylporphyrin

wave at E_{ox}^1 = +0.94 V. This is due to DMF oxidation at high positive potential, resulting in interference with the second oxidation wave of **1**.

With [*N*-methyl-3-pyridyl$^+$]$_4$ and Zn_2–[*N*-methyl-3-pyridyl$^+$]$_4$ in DMF, only one oxidation potential can be observed. Thin-layer coulometric experiments show that the oxidation process involves a single-step 2e$^-$ transfer (eq 2). This indicates that the

$$(MP, MP) \xrightarrow{-2e^-} (MP^{\bullet+}, MP^{\bullet+}) \qquad (2)$$

(MP, MP) = dimeric tetraphenylporphyrin

two porphyrin rings undergo 1e$^-$ oxidation at the same or at very nearly the same potential. Similar behavior is observed in the reduction of [*N*-methyl-3-pyridyl$^+$]$_4$ and Zn_2–[*N*-methyl-3-pyridyl$^+$]$_4$ in DMF. With the cofacial porphyrin dimers [1-naphthyl]$_4$ and Zn_2–[1-naphthyl]$_4$, there are observed two one-electron processes (eq 3). This finding indicates that the two porphyrin

$$(MP, MP) \xrightarrow{-e^-} (MP, MP)^{\bullet+} \xrightarrow{-e^-} (MP^{\bullet+}, MP^{\bullet+}) \qquad (3)$$

rings in [1-naphthyl]$_4$ and Zn_2–[1-naphthyl]$_4$ are sufficiently close to allow strong π–π interactions.[10e,11] The most upfield shifted N–H resonances are observed for [1-naphthyl]$_4$ (Table I). To our knowledge [1-naphthyl]$_4$ and Zn_2–[1-naphthyl]$_4$ represent the only tetraphenylporphyrin dimers which exhibit two discrete 1e$^-$ oxidation CV waves (Table III). Thus, the steric requirement of the 1-naphthyl substituent has changed the conformation of the connecting legs (from a to b in Chart III) bringing about a closer proximity of the porphyrin planes. On the other hand, in [*N*-methyl-3-pyridyl$^+$]$_4$ and Zn_2–[*N*-methyl-3-pyridyl$^+$]$_4$ the two porphyrin rings are at such a distance that they behave as separate entities {compare electrochemical results of [*N*-methyl-3-pyridyl$^+$]$_4$ to that of monomeric porphyrin **1**, Table III}.

The CV for a solution of Co_2–[*N*-methyl-3-pyridyl$^+$]$_4$ in DMF exhibits one oxidation peak at E_{ox} = +0.38 V. By coulometry it was determined that the single potential is associated with a transferred charge of 1.95 ± 0.1 electron per molecule, showing that the two cobalt(II) centers are simultaneously oxidized. The changes in the visible spectrum in the oxidation of Co_2-II/II dimer (Soret band at 409 nm) to Co_2-III/III dimer via 2e$^-$ transfer are similar to that seen with monomeric cobalt tetraphenylporphyrin.[12] Co_2-III/III displays rather narrow and well-defined absorptions in the visible region (Soret band at 428 nm).

Table IV. Electrocatalytic Reduction of Dioxygen by Quadruply *N*,*N*-Dimethylene Sulfonamide Bridged Cofacial Bis(cobalt tetraphenylporphyrins)

compd[a]	$E_{p,cat}$[b]	% H_2O_2[c]	i_{lim}[d]
Co_2–[3-pyridyl·H$^+$]$_4$	+0.10	34	0.94
Co_2–[*N*-methyl-3-pyridyl$^+$]$_4$[1d]	+0.11	30	1.06
Co_2–[*N*-isopropyl-3-pyridyl$^+$]$_4$	+0.11	31	1.05
Co_2–[*N*-benzhydryl-3-pyridyl$^+$]$_4$	+0.12	29	1.06
Co_2–[methyl]$_4$	+0.05	54	0.75
Co_2–[isopropyl]$_4$	+0.04	56	0.74
Co_2–[1-naphthyl]$_4$	+0.10	51	0.79
Co–**1**[1e]	+0.07	70	0.69

[a] See Chart II and text. [b] Dioxygen electrocatalytic peak potential ($E_{p,cat}$ vs SCE) at graphite disk electrode at scan rate 0.1 V s^{-1}. [c] Calculated from % $H_2O_2 = -i_r/Ni_d$, where i_r and i_d are ring and disk limiting current, respectively, and N is the collection coefficient. [d] Limiting current density (mA cm^{-2}) for the reduction of dioxygen at 100 rpm in O_2-saturated solutions.

Electrocatalytic Reduction of Dioxygen. Results using *N*,*N*-dimethylene sulfonamide bridged bis(cobalt tetraphenylporphyrin) catalysts adsorbed onto the surface of a pyrolytic graphite electrode (PGE) (0.1 N aqueous sulfuric acid[1e]) are provided in Table IV. Under the conditions of the experiments, [3-pyridyl]$_4$ is protonated and has four positive charges {[3-pyridyl·H$^+$]$_4$}. Dominance of 4e$^-$ reduction of oxygen ($O_2 \rightarrow 2H_2O$) over 2e$^-$ reduction ($O_2 \rightarrow H_2O_2$) is observed with the tetracationic [*N*-alkyl-3-pyridyl$^+$]$_4$ and [*N*-protonated 3-pyridyl·H$^+$]$_4$. The bulk of the N-substituent of the 3-pyridinesulfonamide moiety of [*N*-alkyl-pyridyl$^+$]$_4$ does not influence the ratio of 2e$^-$/4e$^-$ reduction of oxygen. Taking into account the relationship of stucture and values of % H_2O_2 formation of this (Table IV) and a previous study,[1e] one may conclude that quadruply bridged bis(cobalt tetraphenylporphyrins) can be placed into one of two groups. The most efficient 2e$^-$ electrochemical catalysis of reduction of O_2 (55 ± 5% H_2O_2) is carried out by those compounds in which the bridge structures have no formal charge. The most efficient 4e$^-$ electrochemical catalysis of reduction of O_2 (69 ± 2% H_2O) are those compounds in which the bridge structures have a formal positive charge. The means by which the positive charges increase the efficiency of catalysis of reduction of $O_2 + 4H^+ \rightarrow 2H_2O$ (electrostatic stabilization of intermediates, conformation, etc.) cannot be established with the data of this study.

Effect of the Number of Bridges in Sulfonamide-Bridged Bis(cobalt tetraphenylporphyrins) on the Electrocatalytic Reduction of Dioxygen to Water. We compare here the quadruply bridged Co_2–[3-pyridyl·H$^+$]$_4$,[1e] the two triply bridged isomers Co_2–[3-pyridyl·H$^+$]$_3$(A) and Co_2–[3-pyridyl·H$^+$]$_3$(B),[13] and the symmetrical doubly bridged Co_2–[3-pyridyl·H$^+$]$_2$. The quadruply

(11) (a) Kobayashi, N.; Lam, H.; Nevin, W. A.; Janda, P.; Leznoff, C. C.; Lever, A. B. P. *Inorg. Chem.* **1990**, *29*, 3415. (b) Dewulf, D. W.; Leland, J. K.; Wheeler, B. L.; Bard, A. J.; Batzel, D. A.; Dininny, D. R.; Kenney, M. E. *Inorg. Chem.* **1987**, *26*, 266. (c) Simic-Glavaski, B.; Tanaka, A. A.; Kenney, M. E.; Yeager, E. J. *J. Electroanal. Chem. Interfacial Electrochem.* **1987**, 229, 285.

(12) Ozer, D.; Parash, R.; Broitman, F.; Mor, U.; Bettelheim, A. *J. Chem. Soc. Faraday Trans. 1* **1984**, *80*, 1139.

(13) Karaman, R.; Almarsson, Ö.; Blaskó, A.; Bruice, T. C. *J. Org. Chem.* **1992**, *57*, 2169.

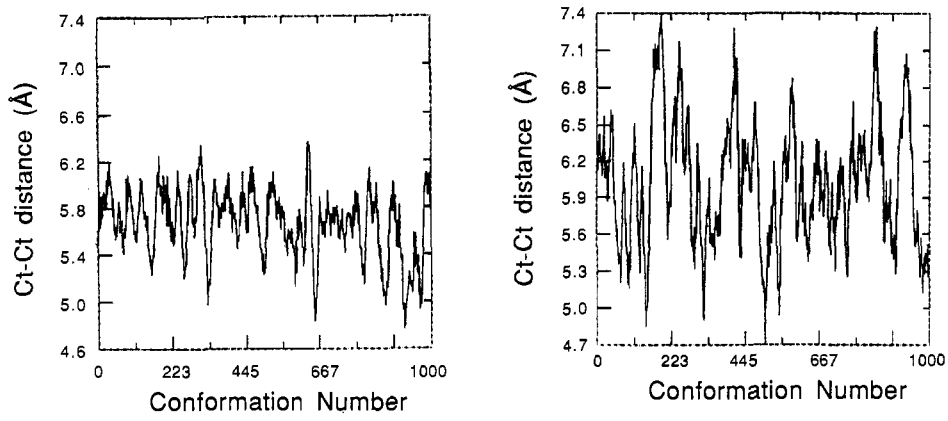

Figure 6. Center to center (Ct–Ct) distance vs dynamics trajectories in $CHARM_m$ simulations of 3-pyridinesulfonamide-linked free-base dimers: (a, left) Quadruply bridged $[3\text{-pyridyl}]_4$; (b, right) doubly strapped $[3\text{-pyridyl}]_2$.

Chart V

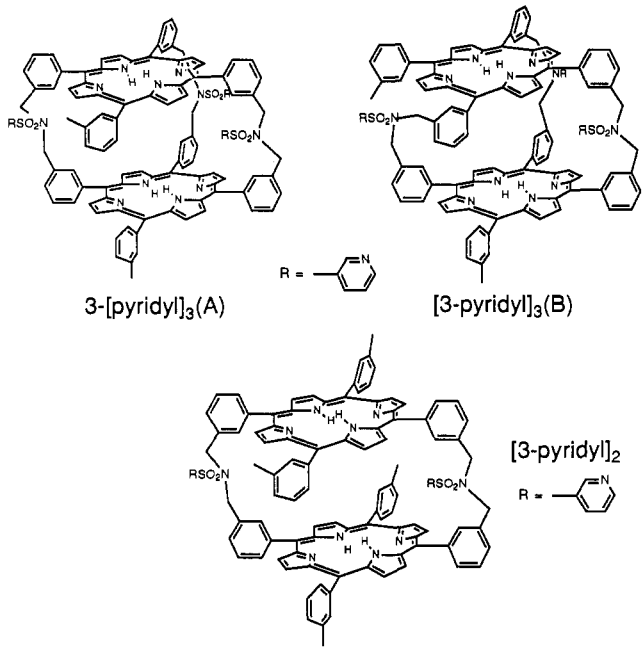

Table V. Effects of the Number of Bridges in *N,N*-Dimethylene Sulfonamide Bridged Bis(cobalt tetraphenylporphyrin) Dimers on Electrocatalytic Reduction of Dioxygen[a]

compd	$E_{p,cat}$	i_{lim}	% H_2O_2	Ct–Ct[b]	P–P[b]	LS[b]
Co_2–[3-pyridyl·H^+]$_2$	+0.04	0.70	67	6.38	5.9	3.0
Co_2–[3-pyridyl·H^+]$_3$(B)	–0.10	0.71	63	6.54[c]	6.3	1.3
Co_2–[3-pyridyl·H^+]$_3$(A)	–0.05	0.76	52	5.57[c]	5.2	1.0
Co_2–[3-pyridyl·H^+]$_4$	+0.10	0.94	34	5.03	5.0	0.2

[a] See Table IV for explanation of column headings. [b] By $CHARM_m$; see Chart I. [c] See ref 13.

bridged cofacial porphyrin dimers are characterized by small values of LS such that P–P essentially equals Ct–Ct (Chart I). This is not so for the triply and doubly bridged cofacial porphyrins. Molecular dynamics calculations of dimers $[3\text{-pyridyl}]_2$, $[3\text{-pyridyl}]_3$(A, B)[13] (see Chart V), and $[3\text{-pyridyl}]_4$ show, as expected, that the flexibility of the dimeric porphyrin is largely dependent on the number of the bridges (Figure 6). From Figure 6 and Table V, the quadruply bridged porphyrin dimer $[3\text{-pyridyl}]_4$ is the most rigid with Ct–Ct distance of 5.0 Å by $CHARM_m$ calculations. The doubly bridged dimer $[3\text{-pyridyl}]_2$ is the most flexible and exhibits the longest Ct–Ct distance (see Figure 6b). The two isomers of the triply bridged dimers $[3\text{-pyridyl}]_3$(A) and $[3\text{-pyridyl}]_3$(B) have moderate flexibility, where the more symmetrical isomer $[3\text{-pyridyl}]_3$(A) has a shorter Ct–Ct distance than $[3\text{-pyridyl}]_3$(B) (5.6 Å vs 6.5 Å).[13]

The results of the electrocatalytic reduction of dioxygen by bis(cobalt porphyrin) dimers Co_2–[3-pyridyl·H^+]$_2$, Co_2–[3-pyridyl·H^+]$_3$(A), Co_2–[3-pyridyl·H^+]$_3$(B), and Co_2–[3-pyridyl·H^+]$_4$ are summarized in Table V. The doubly bridged Co_2–[3-pyridyl·H^+]$_2$ displays catalytic activity similar to that observed for monomeric TPP (Table IV). The triply bridged Co_2–[3-pyridyl·H^+]$_3$(A) and Co_2–[3-pyridyl·H^+]$_3$(B) show more catalytic activity than the doubly bridged dimer. The Co_2–[3-pyridyl·H^+]$_3$(A) is a more effective catalyst than its less symmetric and more extended isomer Co_2–[3-pyridyl·H^+]$_3$(B). The Co_2–[3-pyridyl·H^+]$_4$ yields the most 4e⁻ reduction of O_2. The relationship of % 4e⁻ reduction with molecular dynamics calculated distances (Table V) is not clear, except that, as LS decreases, the % 4e⁻ reduction increases. The order of the dimer flexibility by dynamics calculations {$[3\text{-pyridyl}]_4$ < $[3\text{-pyridyl}]_3$(A) < $[3\text{-pyridyl}]_3$(B) < $[3\text{-pyridyl}]_2$} is that for efficiency of 4e⁻ reduction of dioxygen to water. This is, however, the order for decrease in the number of positive charges on the Co_2–ligated molecules and this feature should also decrease the % 4e⁻ reduction of O_2.

Summary

For the structures of Chart II, the *N,N*-dimethylene alkane- or arenesulfonamide linker moieties may assume folded conformations which bring the two porphyrin rings into close proximity. The relationships among ^1H NMR chemical shifts for pyrrolic N–H protons and (i) molecular mechanics calculated interplanar distances and (ii) Taft's steric parameter E_S reveal that the nature of the alkyl or aryl substituent R on the sulfonamide linkers [$(-CH_2)_2NSO_2R$] influences the interplanar separation. This does not seem to significantly alter the efficiency of this class of cofacial bis(cobalt porphyrin) dimers as catalysts for the electrochemical 4e⁻ reduction of dioxygen to water. We found, however, that the presence of positive charges on the linkers increases the activity of the catalyst. Thus, in a series of [$(-CH_2)_2NSO_2C_5H_5N$–X^+]-bridged dimers, where X is H, CH_3, $CH(CH_3)_2$, or $CH(Ph)_2$, the percentage of 4e⁻ reduction was 69 ± 3%. All other quadruply aza-bridged Co_2–TPP dimers studied by us which have no formal charges show less than 45 ± 6% 4e⁻ reduction of oxygen to water.[14] Finally, reducing the number of bridges between the porphyrin moieties has a detrimental effect on the efficacy for 4e⁻ reduction of O_2 to H_2O. This is possibly due to an increase in structural flexibility [as an increase in LS and a decrease in coplanarity of the porphyrin rings] and/or due to the decreased number of peripheral positive charges, a decrease in a positive electrostatic effect upon the kinetics of O_2 reduction. An exact explanation of the results are probably not possible

(14) The best yield of 4e⁻ reduction of O_2 obtained in this study (~70%) compares unfavorably with the efficiencies observed previously by Collman and Chang (see ref 2) (~95%). A plausible explanation is that we have employed modified tetraphenylporphyrins whereas both Collman and Chang used porphyrin systems with unsubstituted *meso*-carbons.

because the differences observed in the ratio of percentage of $4e^-/2e^-$ reduction are accounted for by less than 1 kcal/mol.

Experimental Section

General Methods. Absorption spectra were recorded on a Cary-14 spectrophotometer interfaced to a Zenith computer, equipped with OLIS (On-Line Instrument System Inc.) data acquisition and processing software. Emission spectra were run on a Perkin-Elmer LS 50 fluorescence spectrophotometer. Fast atom bombardment (FAB) mass spectroscopy was performed at UCSB using *m*-nitrobenzyl alcohol as the matrix and a parallel run of cesium rubidium iodide as the reference. Zn_2–[*N*-methyl-3-pyridyl]$_4$, Co_2–[*N*-methyl-3-pyridyl$^+$]$_4$, Co_2–[3-pyridyl$^+$]$_4$, and Co-1 were prepared as previously reported.[1d,e] All reactions were carried out with purified reagents in dry, purified solvents. Column chromatography was performed with Fischer type 60-Å (200–425 mesh) silica gel. Preparative thin-layer chromatography (TLC) was performed using EM Sciences Kieselgel 60 F_{254}.

NMR experiments were recorded at 500 MHz on a General Electric GN-500 spectrometer at 25 °C in $CDCl_3$. Chemical shifts were reported relative to the signal of $CHCl_3$ (^{1}H, 7.240 ppm). ROESY spectra were collected using the Kessler pulse sequence:[5] $90°_x$–t_1–$(\beta_y$–$\tau)_n$-aquisition. The sample was degassed with argon and sealed. Spectra were collected into 4K data blocks for 512 t_1 increments with a relaxation delay of 3 s, $\beta = 30°$, $\tau = 3$ ms, and $n = 7491$ to give a mixing time of 200 ms with a locking field strength of 2.5 kHz and spectral width in both dimensions of 8333.33 Hz. Data matrix was zero filled to 2 K and apodized with a Gaussian function to give a line broadening in both dimensions of 4 Hz. The 2D spectrum was reversed to transform the negative ROESY peaks into positive ones, and the volume integrals of the peaks were measured. Quantitative data were obtained using eq 4, which includes also the offset

$$r^6_{ab} = K \sin^2(\beta_a) \sin^2(\beta_b)/I_{ab}$$

$$\beta_i = \text{arctg}(\gamma B_1/\omega_i) \qquad (4)$$

correction, where r_{ab} is the distance between protons a and b, B_1 is the field strength of the locking field, γ is the magnetogyric ratio, ω_i is the resonance offset of nucleus i, and K is a constant evaluated from the cross peaks volume integral I_{ij} of protons i and j with a known separation.

Electrochemistry. Cyclic voltammetric measurements were performed with a three-electrode potentiostat (Bioanalytical Systems, Model CV-27) and were recorded on Houston Instruments Model 100 Omnigraphic. A platinum-wire electrode separated from the analyte compartment by a medium-porosity glass frit was used as the auxiliary electrode. A Ag/AgCl electrode, filled with aqueous tetramethylammonium chloride solution and standardized to 0.00 V vs SCE, with a solution junction via a Pyrex-glass tube closed with a soft glass cracked bead contained in a luggin capillary, was used as the reference electrode. A platinum disk electrode (1.0-mm diameter) was employed as the working electrode. Rotating ring-disk experiments were conducted using an RDE4 instrument (Pine Instrument Co.). Pyrolytic graphite disk/platinum ring electrodes were used. The ring collection efficiency ($N = 0.17$) was determined using the potassium iodide acid solution.[1e] All working electrode surfaces were highly polished with alumina paste prior to each experiment. Adsorption of porphyrins was performed by dropping organic solvents containing porphyrin on the disk electrode, followed by careful evaporation of the solvent. Dioxygen concentrations in O_2-saturated solutions were assumed to be 1.2 mM at room temperature. H_2SO_4 solutions of 1 N concentration were used as supporting electrolytes. All reported potentials are with respect to saturated calomel electrode (SCE).

Theoretical and Distance Geometry Calculations. All model building and calculations were performed on a Silicon Graphics IRIS 4D/220 GTX workstation, using the programs Quanta, version 3.2 (MSI), and $CHARM_m$,[6] version 21.3. The topology file PORPHYRINH.RTF supplied by MSI was used as a basis for the porphyrin moieties of the dimers, and the linkers were constructed in Chemnote, the 2D modeling facility in Quanta. Minimizations were performed using steepest descent algorithm and parameter file PARM30.BIN, followed by adopted basis Newton–Raphson algorithm, until the energy change tolerance was less than 10^{-9} kcal/mol. Nonbonded interaction cutoff distance and hydrogen bonding cutoff distance were chosen to be 11.5 and 7.5 Å, respectively. Molecular dynamics were performed using Verlet integration and the SHAKE algorithm to fix X–H bonds. At 600 K, the maximum allowable fluctuation in temperature was fixed at 25°. Nonbonded interaction and hydrogen bond lists were updated every 0.05 ps/step.

The distance geometry (DGEOM) program was supplied by Du Pont de Nemours and uses an algorithm already reported.[15] The ROESY distance constraints were input using a constraints file, and the RMSFIT.MATRIX was cluster analyzed using a program Data Desk[8] (Odesta Corp.).

Synthetic Procedures. Preparation of [1-naphthyl]$_4$, [isopropyl]$_4$, and [methyl]$_4$. The dimers were prepared by methods analogous to that used to synthesize [3-pyridyl]$_4$.[1e] Two equivalents of the corresponding sulfonamides (methanesulfonamide was purchased from Aldrich; isopropyl and 1-naphthyl sulfonamides were prepared by ammonolysis of the sulfonyl chlorides from Aldrich) were alkylated with 1 equiv of **1** for 24 h in DMF (1×10^{-3} M porphyrin monomer) in the presence of 6 equiv of cesium carbonate. The solution was kept under argon and shielded from light. The solid formed during reaction was filtered off, and evaporation of the filtrate yielded residues which were subjected to flash column chromatography on silica gel, eluting with 0.5% triethylamine in chloroform. The fast and intermediate fractions were combined and further purified by preparative TLC on $0.5 \times 20 \times 20$ cm silica gel plates (E Merck).

[1-naphthyl]$_4$: TLC eluent 0.5% methanol in chloroform. The fourth band ($R_f = 0.67$) was isolated: Yield 6%; FABMS m/z 2152 (calcd for $C_{136}H_{100}N_{12}O_8S_4$ [M$^+$] m/z 2152.5); UV/vis ($CHCl_3$) λ_{max} ($\epsilon \times 10^{-3}$ cm^{-1} M^{-1}) 406 (sh), 414 (333), 513 (20.2), 550 (13), 589 (9.9), 645 (7.1); ^{1}H NMR ($CDCl_3$) δ (ppm) 8.92 (d, $J = 7.5$ Hz, 4H), 8.87 (d, $J = 7.5$ Hz, 4H), 8.56 (d, $J = 7.5$ Hz, 4H), 8.45 (d, $J = 7.5$ Hz, 4H), 8.24 (t, $J = 7.5$ Hz, 8H), 8.19 (d, $J = 7.5$ Hz, 8H), 8.17 (s, 16H, β-pyrrolic), 8.09 (dd, $J = 7.5$ Hz, 8H), 7.89 (dd, $J = 7.5$ Hz, 8H), 7.73 (dd, $J = 7.5$ Hz, 4H), 7.68 (dd, $J = 7.5$ Hz, 4H), 7.61 (dd, $J = 7.5$ Hz, 4H), 7.53 (dd, $J = 7.5$ Hz, 8H), 4.77 (s, 16H, bridging CH_2), –4.68 (broad s, 4H, pyrrolic N–H). The purple third band immediately ahead of the desired product was found, by MS and ^{1}H NMR, to be the mono(zinc) derivative of the dimer, which could be isolated and either treated with trifluoroacetic acid to give [1-naphthyl]$_4$ or with zinc salts to yield Zn_2–[1-naphthyl]$_4$. The fastest band was found to be the mono(carbonate) tris(1-naphthyl–NSO_2) linked dimer (see ref 4).

[isopropyl]$_4$: TLC eluent 1.0% methanol in chloroform. The third band ($R_f = 0.47$) was isolated: Yield 3%; FABMS m/z 1813 (calcd for $C_{108}H_{92}N_{12}O_8S_4$ [M$^+$] m/z 1812.6); UV/vis ($CHCl_3$) λ_{max} ($\epsilon \times 10^{-3}$ cm^{-1} M^{-1}) 404 (sh), 415 (201), 513 (16), 549 (13), 590 (9.0), 643 (7.9); ^{1}H NMR ($CDCl_3$) δ (ppm) 8.25 (s, β-pyrrolic, 16H), 7.99 (d, $J = 7.5$ Hz, 8H), 7.95 (d, $J = 7.5$ Hz, 8H), 7.72 (t, $J = 7.5$ Hz, 8H), 7.30 (s, 8H), 4.69 (s, 16H, bridging CH_2), –4.28 (broad s, 4H, pyrrolic N–H). The second band was found to be the mono(carbonate) tris(isopropyl–NSO_2) linked dimer (see ref 4).

[methyl]$_4$: TLC eluent 1.0% methanol in chloroform. The fourth band ($R_f = 0.31$) was isolated: Yield 3%; FABMS m/z 1706 (calcd for $C_{100}H_{79}N_{12}O_8S_4$ [M$^+$] m/z 1706.5); UV/vis ($CHCl_3$) λ_{max} ($\epsilon \times 10^{-3}$ cm^{-1} M^{-1}) 403 (sh), 415 (169), 513 (15), 549 (11), 589 (9.5), 643 (8.1); ^{1}H NMR ($CDCl_3$) δ (ppm) 8.29 (s, β-pyrrolic, 16H), 8.17 (d, $J = 7.5$ Hz, 8H), 8.03 (d, $J = 7.5$ Hz, 8H), 7.74 (t, $J = 7.5$ Hz, 8H), 7.30 (s, 8H), 4.69 (s, 16H, bridging CH_2), –4.03 (broad s, 4H, pyrrolic N–H). The third band was found to be the mono(carbonate) tris(methyl–NSO_2) linked dimer (see ref 4).

Preparation of Co_2–[1-naphthyl]$_4$, Co_2–[methyl]$_4$, Co_2–[isopropyl]$_4$, Co_2–[3-pyridyl]$_2$, Co_2–[3-pyridyl]$_3$(A), and Co_2–[3-pyridyl]$_3$(B). A mixture of [1-naphthyl]$_4$, [methyl]$_4$, [isopropyl]$_4$, [3-pyridyl]$_2$, [3-pyridyl]$_3$(A), or [3-pyridyl]$_3$(B)[1,13] (0.024 mmol) and $CoCl_2 \cdot 6H_2O$ (50 mg, 0.21 mmol) in DMF (10 mL) was heated at 130 °C for 12 h and then diluted with chloroform (100 mL). The reaction mixture was extracted with water and brine, dried over anhydrous Na_2SO_4, filtered, and evaporated to yield a deep orange powder. The orange material was subjected to silica gel column eluting with mixtures of chloroform/methanol, and the nonpolar orange band was collected.

Co_2–[1-naphthyl]$_4$: Yield 95%; FABMS m/z 2275 (calcd for $C_{136}H_{98}N_{12}O_8S_4Co_2$ [M$^+$] m/z 2274.6); UV/vis (DMF) λ_{max} ($\epsilon \times 10^{-3}$ cm^{-1} M^{-1}) 420 (142), 550 (11.6).

Co_2–[methyl]$_4$: Yield 90%; FABMS m/z 1821 (calcd for $C_{100}H_{79}N_{12}O_8S_4Co_2$ [M$^+$] m/z 1821.4); UV/vis (DMF) λ_{max} ($\epsilon \times 10^{-3}$ cm^{-1} M^{-1}) 414 (445), 514 (22.2).

(15) (a) Crippen, G. M. In *Distance Geometry and Conformational Calculations*; Bawden, D., Ed.; Research Studies Press, John Wiley: New York, 1981. (b) Havel, T. F.; Kunoto, I. D.; Crippen, G. M. *Bull. Math. Biol.* **1983**, *45*, 665.

Co_2–[isopropyl]$_4$: Yield 89%; FABMS m/z 1930 (calcd for $C_{108}H_{92}N_{12}O_8S_4Co_2$[$M^+$] m/z 1930.5); UV/vis (DMF) λ_{max} ($\epsilon \times 10^{-3}$ cm^{-1} M^{-1}) 409 (270), 530 (33.5).

Co_2–[3-pyridyl]$_2$: Yield 93%; FABMS m/z 1763 (calcd for $C_{106}H_{76}N_{12}O_4S_2Co_2$ [M^+] m/z 1762.4); UV/vis (DMF) λ_{max} ($\epsilon \times 10^{-3}$ cm^{-1} M^{-1}) 412 (350), 530 (24.6).

Co_2–[3-pyridyl]$_3$(A): Yield 87%; FABMS m/z 1917 (calcd for $C_{111}H_{78}N_{14}O_6S_3Co_2$ [M^+] m/z 1916.4); UV/vis (DMF) λ_{max} ($\epsilon \times 10^{-3}$ cm^{-1} M^{-1}) 409 (307), 530 (19.5).

Co_2–[3-pyridyl]$_3$(B): Yield 94%; FABMS m/z 1917 (calcd for $C_{111}H_{78}N_{14}O_6S_3Co_2$ [M^+] m/z 1916.4); UV/vis (DMF) λ_{max} ($\epsilon \times 10^{-3}$ cm^{-1} M^{-1}) 410 (317), 530 (22.4).

Preparation of Co_2–[*N*-isopropyl-3-pyridyl$^+$]$_4$ and Co_2–[*N*-benzhydryl-3-pyridyl$^+$]$_4$: A mixture of [*N*-isopropyl-3-pyridyl$^+$]$_4$ or [*N*-benzhydryl-3-pyridyl$^+$]$_4$[I] (0.01 mmol) and $CoCl_2 \cdot 6H_2O$ (50 mg, 0.21 mmol) in DMF (5 mL) was heated at 135 °C for 6 h. The reaction mixture was evaporated, and the resulting green residue was triturated with cold water, filtered out, washed with ether, and dried.

Co_2–[*N*-benzhydryl-3-pyridyl$^+$]$_4$: Yield 97%; FABMS m/z 2571 (calcd for $C_{155}H_{113}N_{16}O_8S_4Co_2$ [M^+ – benzhydryl] m/z 2571.6); UV/vis (DMF) λ_{max} ($\epsilon \times 10^{-3}$ cm^{-1} M^{-1}) 410 (310), 530 (23.5).

Co_2–[*N*-isopropyl-3-pyridyl$^+$]$_4$: Yield 94%; FABMS m/z 2199 (calcd for $C_{125}H_{101}N_{16}O_8S_4Co_2$ [M^+ – isopropyl] m/z 2199.6); UV/vis (DMF) λ_{max} ($\epsilon \times 10^{-3}$ cm^{-1} M^{-1}) 410 (280), 530 (27.7).

Preparation of Zn_2–[1-naphthyl]$_4$. To a methanolic (2 mL) solution of potassium acetate (30 mg, 0.31 mmol) and zinc acetate dihydrate (30 mg, 0.14 mmol) at room temperature was added a solution of [1-naphthyl]$_4$ (20 mg, 9.0 μmol) in 1 mL of chloroform. The resulting solution was stirred under argon in the dark for 12 h. The product was isolated by adding chloroform (20 mL) and water (20 mL), separating the layers, and reextracting the aqueous layer with chloroform (10 mL). The combined chloroform was washed with water and brine and dried over anhydrous sodium sulfate. Filtration and evaporation afforded 17 mg of Zn_2–[1-naphthyl]$_4$ (82%) as a purple powder. TLC (SiO_2, eluent $CHCl_3$) indicated only one porphyrin product: FABMS m/z 2284 (calcd for $C_{136}H_{96}O_8N_8S_4Zn_2$ [$M^+ + 4H^+$] m/z 2284.9); UV/vis ($CHCl_3$) λ_{max} ($\epsilon \times 10^{-3}$ cm^{-1} M^{-1}) 405 (sh) (733), 412 (871), 515 (11.4), 552 (25.2), 592 (9.4); ^1H NMR ($CDCl_3$) δ (ppm) 8.60 (d, J = 7.5 Hz, 4H), 8.29 (d, J = 7.5 Hz, 4H), 8.06 (d, J = 7.5 Hz, 4H), 8.00 (s, 16H, β-pyrrolic), 7.95 (d, J = 7.5 Hz, 4H), 7.68 (t, J = 7.5 Hz, 4H), 7.61 (t, J = 7.5 Hz, 4H), 7.53 (t, J = 7.5 Hz, 4H), 4.77 (s, 16H, bridging CH_2).

Acknowledgment. This study was supported by grants from the National Institutes of Health and Chiron Corp. of Emeryville, CA.

Supplementary Material Available: Table SI, an x, y, z coordinates file of the 2D NMR solution structure for dimer [3-pyridyl]$_4$ (4 pages). Ordering information is given on any current masthead page.